Combined wavelet transforms and neural network feed-forward model for ECG peak detection and classification

Raghavendra Badiger, Prabhakar Manickam
Department of Computer Science and Engineering, REVA University, Bengaluru, India

Article Info

ABSTRACT

We have focused on development of a combined approach for electrocardiogram (ECG) signal filtering and various ECG peak detection. The filtering model is based on the combination of wavelet transform and neural network where after computing the wavelet coefficients the neural network feed-forward model is used to update the weights. The filtered signal is processed through the convolution layers and bidirectional long short-term memory (Bi-LSTM) architecture to perform the ECG peak detection. Further, we apply a combined feature extraction strategy where wavelet transform and morphological feature are extracted to classify the ECG beats as classify 5 different types of heartbeats, including premature ventricular contraction (PVC), left bundle branch block (LBBB), right bundle branch block (RBBB), PACE, and atrial premature contraction (APC) to examine the heart condition. The feature extraction phase uses wavelet transform, morphological features and high-order statistics to generate the robust features. The obtained feature vector is processed through the principal component analysis (PCA) module to reduce the dimension of feature vector. These features are trained by using support vector machine (SVM) and k-nearest neighbor (KNN) supervised model. The proposed approach is tested on publicly available MIT-BIH dataset where performance analysis shows that the proposed approach obtained average precision, sensitivity and error as 99.98%, 99.96%, and 0.101 which outperforms the existing filtering and peak detection schemes.

This is an open access article under the CC BY-SA license.

Corresponding Author:

Raghavendra Badiger
Department of Computer Science and Engineering, REVA University
Rukmini Knowledge Park, Yelahanka, Antigenically, Bengaluru, Karnataka 560064, India
Email: raghavendra.badiger1@gmail.com

1. INTRODUCTION

According to World Health Organization (WHO), the coronary artery diseases (CaDs) are considered as one of the leading causes of mortality by causing about 17.9 million fatalities every year. Coronary heart diseases account for 80% of these fatalities which includes several heart diseases such as heart attack, and cerebrovascular illness [1]. Moreover, a study presented in [2] has reported that the middle aged and elderly people are the most vulnerable. Kishore and Michelow [3] WHO has projected the increased death count up to 23.4 million by 2030. Therefore, early detection of this type of diseases can help to prevent the mortality by providing efficient diagnosis. Currently, several advanced health monitoring systems are being developed to improve the quality of health monitoring. Moreover, the technological advancements have proliferated the need to upgrade these systems. A key barrier to raising the standard of medical care is the lack of physicians or medical equipment, as well as the distance between the doctors and the patients. The possibility of routine health examinations in such circumstances is also problematic [3]. Therefore,

development of portable health monitoring systems has become one of the important factors in health monitoring applications. Several health monitoring systems have been developed such as smartwatch, health bands, and sensors.

Figure 1 shows structure of heart and wave generation of electrocardiogram (ECG). Heart structure is depicted in Figure 1(a) with specialized cells and nodes that control heartbeat. These advancements are also adopted in monitoring the heart conditions by monitoring the ECG signals. These signals are helpful in recording the electrical activities of human heart during the depolarization and repolarization process of heart muscles. According to this process, a normal rhythm "sinus rhythm" originates from the sinoatrial (SA) node and extents toward the atrioventricular (AV) node due to the contraction of atria resulting in forcing the blood into the ventricles. The atria are the upper chamber of heart and its activation is represented by P-wave. Further, these ventricles contract and pump the blood out of the heart as electrical signal reach the ventricular muscle cells. Here, the QRS complexes characterize the activation of ventricles. Next, in order to prepare for the subsequent heartbeat, the ventricles must go through an electrical shift. The T wave, which is a representation of this electrical activity, is known as the recovery wave, Figure 1(b) shows this process.

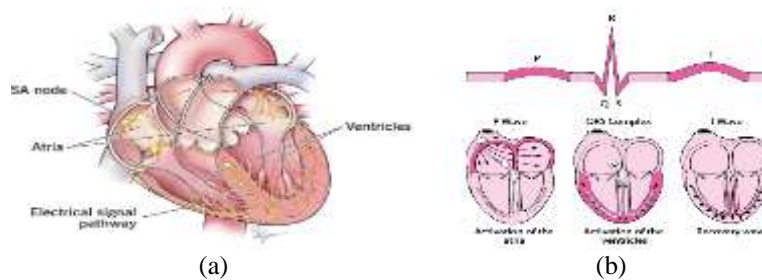(a)   (b)

Figure 1. Structure of heart and electrical activity (a) heart structure and (b) ECG wave generation

ECG is a non-invasive approach to depict the significant electrical information of heart collected by employing the electrodes tied on the human body. In order to improve the electrical performance analysis of heart, these electrodes are made of non-noble metals. In a 12-lead system, 4 electrodes are placed in the right and left limbs, and 6 other electrodes are placed on different points of the chest. This arrangement of 10 electrodes is shown in Figure 2. A typical 12-lead ECG system is presented in Figure 2(a) which contains three limbs named as I, II, and III. Similarly, it contains six chest leads which are designated form V1 to V6 and three augmented limbs as presented in Figure 2(b). The appropriate analysis of ECG signals can be helpful in detecting several heart related abnormalities such as arrhythmia, heart attack, heart failure, and hypertrophy. The leads measure the electrical potential at one electrode in order to determine the lead I, lead II, and lead III patterns. This is spatially represented by an Einthoven's triangle, which is depicted in Figure 2(c).

(a)   (b)
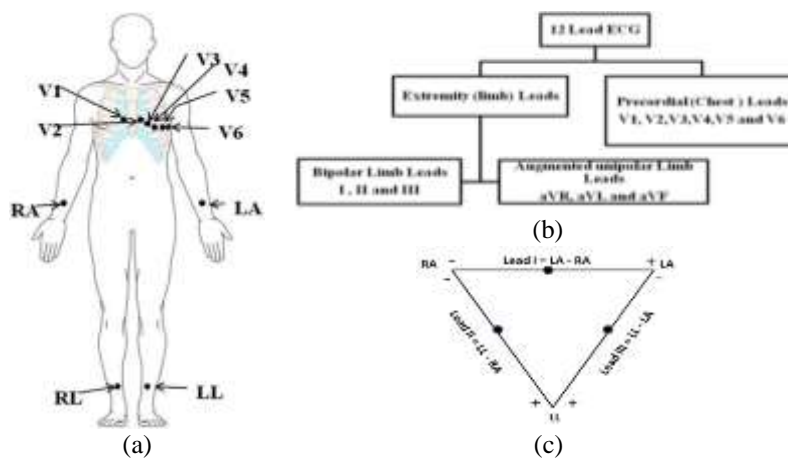   (c)

Figure 2. Arrangement of 10 electrode: (a) electrode placement, (b) 12 lead ECG, and (c) Einthoven's triangle to describe the placement

Generally, these signals are contaminated during acquisition process due to different types of noises. Most popular noise types which affect the signal quality are: base line wander (0.15-0.3 Hz) [4], power line interference [5], muscle artefacts [6], [7]. Baseline wander and PLI are the most prominent noises that alter and substantially distort the diagnostic data included in an ECG signal. In order to prevent incorrect evaluations and to increase the diagnostic accuracy, these artefacts must be eliminated.

Similarly, in ECG signals, cardiac cycles present several events in the forms of waveforms such as P wave, QRS complex, R peak, and T wave. Accurate detection and localization of these peaks plays important role in classification of heart conditions. Therefore, ECG signal filtering and peak detection are considered as the primary important tasks in ECG signal processing. Several methods have been developed to eliminate the noise from ECG signals to improve the quality of analysis. However, Wavelet transform based methods have been considered as promising technique because of its nature to represent the non-stationary signal efficiently and dividing the signal into different frequency bands [8]. Traditional methods have adopted smoothing filtering methods to obtain the denoised ECG signals such as Acharya *et al.* [9] used SavitzkyGolay filtering, Sarafan *et al.* [10] presented extended Kalman filter (EKF), Dwivedi *et al.* [11] presented a combined model by using wavelet and empirical mode decomposition (EMD), Ding *et al.* [12] presented recursive least squares (RLS). Current advancements in artificial intelligence have led to develop the advanced machine learning concepts, motivated by this, neural network-based models are also adopted for filtering the ECG signal such as deep convolution neural network (CNN) for denoising the fatal ECG [13], encoder decoder based deep learning model [14], autoencoder [15]. Similarly, several peak detection methods also have been presented such as Pan-Tompkin's algorithm, wavelet transform, and Hilbert transform. However, the deep learning-based approaches have gained huge attention in this domain. Jang *et al.* [16] presented CNN based peak detection by splicing the segmentation and regression modules, Zahid *et al.* [17] presented 1D CNN model for R peak detection. This description shows that several works have been introduced such as SavitzkyGolay filtering, EKF, EMD, RLS, machine learning, and deep learning such as autoencoder models. Despite of several advanced techniques combined denoising and peak detection with substantial accuracy remains a challenging task. Moreover, the existing methods focused on limited noise types whereas the real-time environment suffer from different types of noises. This causes issues while generalizing the model for ECG signal processing.

Therefore, in this work, we adopt the deep learning concept and presented a combined model for ECG signal filtering and peak detection. In filtering phase, we adopted wavelet-based approach and combined the coefficient updating process with neural network's feed forward process. Once the signal is filtered, we process it through the convolution layers and bidirectional long short-term memory (Bi-LSTM) network module to obtain the final peak locations. In next stage, a hybrid feature extraction technique is implemented which uses wavelet transform, morphological filters and high order statistics feature. The obtained features are process through the principal component analysis (PCA) based dimension reduction scheme. Finally, the reduced dimension features are processed through the supervised machine learning process to classify the different beats. Rest of the article consist of following sections: section 2 presents the brief literature review about ECG filtering and peak detection, section 3 presents the proposed deep learning based combined solution to achieve the filtered signal along with its peaks, section 4 presents the comparative analysis of proposed model and finally, section 4 presents the concluding remarks and future scope for ECG processing.

2. METHOD

This section presents a detailed literature review. It will discuss ECG filtering techniques and peak detection and classification and a proposed solution for combined ECG filtering, peak detection and classification using a supervised machine learning approach. Here are the details:

2.1. Literature survey

In previous section, we have described the advancement in health monitoring system, importance of ECG signal, evolution of machine and deep learning-based methods for bio-medical signal analysis. In order to obtain the precise analysis of ECG signals, denoising the ECG signal and detection of peaks play important role. Several researches have been conducted to accomplish this task. This section presents a brief discussion on existing techniques of ECG filtering and peak detection.

2.1.1. ECG filtering techniques

Kumar *et al.* [18] discussed that ECG-signals are non-stationary in nature therefore noise removal from these signals remains a challenging issue. Therefore, authors studied several filtering techniques such as EMD, low-pass and high-pass filtering. To overcome the drawbacks of these methods, authors adopted the wavelet transform based approach and presented stationary wavelet transform filtering scheme.

Hesar and Mohebbi [19] reported that the model-based methods are important in achieving the significant filtering performance because these methods are realized according to the morphological characteristics of ECG signal. Kalman and EKF are the widely adopted morphological operation-based filtering methods. However, these methods suffer from various challenges such as variations in the morphology, calculation of Kalman filter parameters, and complex noise estimation process. To overcome these issues, authors adopted model-based Bayesian framework and presented adaptive Kalman filter. This model doesn't require any predefined morphological model and it adapts the morphological information automatically. The filter bank used in this model is comprised of two adaptive Kalman filters where first model is used for denoising the QRS complex and another model is used for denoising the Pan and Tompkins (P&T) waves. Moreover, expectation maximization algorithm is used for updating the parameters iteratively and Bryson and Henrikson's technique is used for prediction. Similar to this concept, Sarafan et al. [10] presented ECG denoising approach by using ensemble Kalman filter. However, the traditional Kalman filtering based method have drawback of approximating the posterior probability density of parameters by gaussian distribution. However, if the posterior density in not gaussian sequential monte carlo (SMC) methods achieve better performance.

Mourad [20] introduced ECG filtering technique to handle the wideband type of noise. According to this approach, clean ECG data is modeled by using a combination of different components. Characteristics of these components such as disjoint nature in time domain, overlapping coefficient, and different bandwidths. In order to filter this wide-band noise, authors developed a successive local filtering approach. According to this filtering approach, a segmentation model is developed which produces signal segments with the dominant component. These dominant components are processed through the successively denoising the segmented components by using filters which are designed by penalizing the least-square objective function.

Malik et al. [21] focused on power-line and baseline wander noise from ECG signals. To overcome this, authors presented a hybrid strategy by combining iterative filtering and lifting wavelet transform (LWT). Several researchers have focused on considering the EMD method for filtering but the iterative filtering facilitates appropriate mathematical computations and convergence. The noisy signal generated from iterative filtering is fed to the LWT which is helpful in producing the detailed and approximation coefficients. Further, thresholding method is applied to generate the filtered signal.

2.1.2. Peak detection and classification

ECG peak detection is also considered as an important aspect of ECG signal analysis. Several methods have been presented for efficient peak detection. The main aim of these methods is to reduce the false positive in peak detection.

P&T is considered as a benchmark scheme for ECG filtering. Later, this method was enhanced with the help of Hamilton algorithm which incorporated the performance of P&T method with the help of optimized decision rule process [17]. Similarly, transform domain-based methods are also adopted where wavelet transform, Hilbert transform, modified Hilbert transform with detection threshold, and EMD based schemes.

These methods are divided into two main components as: R-peak enhancement and detection of peaks. In R-peak enhancement phase, several pre-processing techniques are employed such as filter bank and spectral analysis. These techniques are also considered as feature extraction techniques. On the other hand, the detection stage performs decision making with the help of threshold of R-wave. These algorithms are lightweight in nature therefore easily employed in wearable devices. However, these methods perform well on high quality and clean ECG signals and their filtering performance is not robust to the noisy signals. Moreover, performance of these methods deteriorates for high dynamic and noisy ECG signals.

Recently, artificial intelligence has gained huge attention due to their robust learning and classification performance. Several schemes have been presented for peak detection such as Gabbouj et al. [22] introduced 1D self-organized operation neural network (self-ONN). This model consists of generative neurons. Moreover, the self-ONNs have advantage over ONNs because it reduces the need of search of best operator. This model generates the optimal operator during training process.

Similarly, several deep learning based methods have been developed such as Laitala et al. [23] adopted LSTM model for R-peak detection. In this work, authors presented a data generator module to produce the noisy signal to training the LSTM. The LSTM helps to facilitate the temporal modelling to provide the long-term dependencies. Zahid et al. [17] proposed 1D CNN based model for R-peak detection from Holter ECGs. This method shows a significant performance improvement for MIT-BIH dataset but it still suffers from various drawbacks such as: it consists of 12-layer deep learning architecture which increases complexity, and false-positive and false-negatives are still high. Jang et al. [16] focused on the UNet architecture for multiclass semantic segmentation and adopted it in ECG signal processing. This approach has superior performance for QRS complex detection but it predicts around the true peak.

Therefore, additional operations required to detect the entire peaks. In this work, authors adopted regression method to detect the R-peak to ensure the correct location prediction of the peak.

2.2. Proposed method

This section presents the proposed solution for combined ECG filtering, peak detection and classification by using supervised machine learning approach. The complete proposed methodology performs certain steps which are described as in Figure 3:

− Filtering: previous section has described that during acquisition, ECG signals gets contaminated due to some unwanted signals which degrade the quality of original signals resulting in deteriorating the diagnosis performance. Therefore, filtering process is required to remove the noise components. In this work, we use wavelet transform and neural network-based model for this task.

− Peak detection: it plays important role in ECG analysis by detecting various peaks which are useful in examining the exact hear conditions. These peaks are also useful in classifying the ECG patterns as normal ECG or abnormal ECG beats.

− Feature extraction: it plays important role to increase the accuracy of ECG abnormal and normal beat classification. In this work, we adopt wavelet-based coefficients, morphological features and high-order statistical features to formulate the robust feature vector.

− Classification: it is the final stage where we used the extracted features to train the supervised machine learning model. The machine learning model uses certain features and their corresponding labels to produce the trained model which can be used further for classifying the unknown ECG signal.
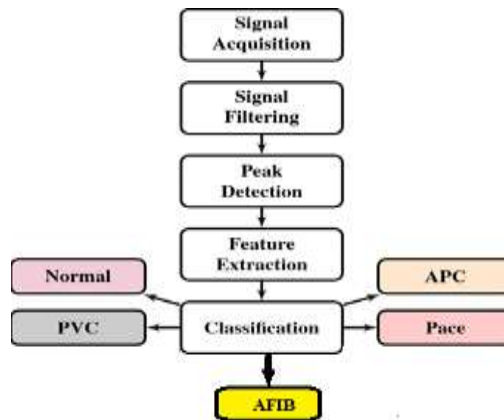

Figure 3. Overall process of proposed model

2.2.1. WaveNet filtering and feature extraction

Literature review section has described the importance of wavelet transform in ECG signal processing. Therefore, it is widely adopted in ECG filtering tasks. Some of the key advantages are as follows:

− It facilitates significant time-frequency localization property.

− It has multi-resolution property which provides the non-stationary characteristics of the signal.

According to the wavelet domain processing, the input signal for processing and processed output signal depends on the function ψ which is known as mother wavelet. The wavelet coefficient can be expressed as (1).

$$f_{j,k} = \int_{-\infty}^{\infty} f(t)\psi_{j,k}(t)\, dt \tag{1}$$

However, computing the coefficients at every scale generates lot of data therefore researchers have adopted the high pass and low-pass filtering concept to compute the expansion of wavelet. The wavelet analysis can be simplified with the help of an auxiliary function $\varphi(t)$ which is called as scaling function which is used to define the approximations. This can be expressed as (2).

$$\varphi_{j,k}(t) = 2^{-\frac{j}{2}}\varphi\left(\frac{t-k2^{j}}{2^{j}}\right) where\ j, k, \in Z \tag{2}$$

This scaling function satisfies the wavelet condition $\int_{-\infty}^{+\infty} \varphi(t)dt = 1$ and two scale difference which can be expressed as (3).

$$\varphi(t) = \sqrt{2} \sum_{k=0}^{L-1} h_k \varphi(2t - k), \text{ where } j, k \in Z \tag{3}$$

Where Z denotes the set of integers.

In order to realize the computations of wavelet transform, a pair of filters is used where one pair of filters is used to compute the wavelet coefficients and other filter pair is used to apply the scaling function. As mentioned before, the scaling function with filter coefficients helps to obtain the approximation. This can be expressed as (4).

$$W_L(n,j) = \sum_m W_L(m, j - 1)h(m - 2n) \tag{4}$$

Similarly, the low high signal can be expressed as (5).

$$W_H(n,j) = \sum_m W_L(m, j - 1)g(m - 2n) \tag{5}$$

Where $W_L(p, q)$ represents the pth scaling coefficient at q^{th} stage, and $W_H(p, q)$ represents the pth wavelet coefficient at q^{th} stage, $h(g)$ represents the scaling or low-pass filter coefficient and wavelet or high pass filter coefficients respectively. The relation between high pass and low pass filter can be expressed as (6). Figure 4 shows the wavelet transform architecture for coefficient extraction.

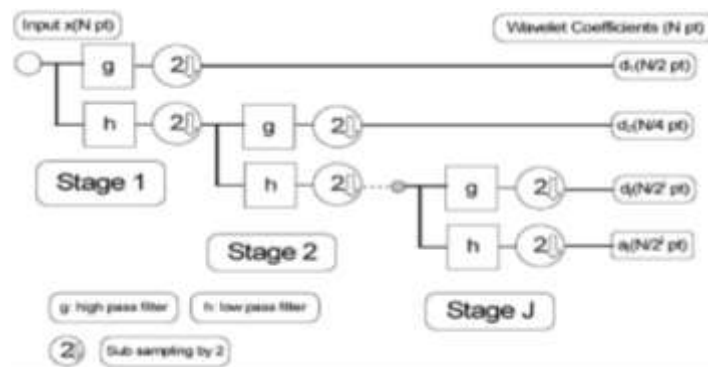$$g_k = (-1)^k h_{L-k}, \dots k = 0, \dots, L - 1 \tag{6}$$

Figure 4. Wavelet coefficient extraction

Further the wavelet transform uses thresholding operations to perform the denoising operations. Generally, two threshold methods are presented in literature: (a) soft thresholding and (b) hard thresholding. The soft thresholding removes the wavelet coefficients which are below the threshold but scales other coefficients. Similarly, the hard thresholding removes the coefficients that are smaller than the defined threshold and other threshold are kept unchanged. Let D is the thresholding operator and λ is the threshold, then we have as (7).

$$z = D(w, \lambda) \tag{7}$$

Where z denotes the wavelet coefficient after thresholding. The filtered signal can be reconstructed by applying inverse wavelet transform as (8).

$$y = T^{-1}(z) \tag{8}$$

In this work, we adopt the machine learning concept and combined the neural network-based process with DWT. The wavelet transform helps to decompose the signal into corresponding wavelet coefficients. The current studies have reported the significant performance of Daubechies wavelet for ECG feature extraction. Therefore, we have adopted Daubechies wavelet in this work.

After achieving the coefficients, the sub band thresholding operations are performed which helps to discard the high-frequency noise and extract the features which are used during the learning process of neural network. It helps to reduce the redundant information for neural network to process. However, the wavelet coefficients still contain some noise due to overlapping of the signals. The neural network helps to minimize these noise parameters by applying the adaptive learning mechanism. Similarly, neural network also participates in the inverse DWT process to generate the output. In this process, neural network compared the filtered output with noise-free signals to update the weights of neural network. To achieve this, the objective function is minimized as (9).

$$J = \frac{1}{2N}\sum_{i=1}^{N}[e(i)]^2 = \frac{1}{2N}\sum_{i=1}^{N}[d(i) - y(i)]^2 \tag{9}$$

Where d represents the desired output and y is the predicted output of neural network, e is the error, and N denotes the total number of outputs. Neural network weights are updated with the help of back-propagation algorithm which is expressed as (10).

$$W(k + 1) = W(k) + \eta\frac{\partial J}{\partial W} \tag{10}$$

Where η denotes the learning rate of the network. Further, the signal is normalized in the interval of [-1, +1] as (11).

$$x_{norm}(t) = 2\left(\frac{x(t) - \hat{x}_{min}}{\hat{x}_{max} - \hat{x}_{min}}\right) - 1 \tag{11}$$

Where $x(t)$ represents the amplitude of signal, x_{norm} is the amplitude of normalized signal, $\hat{x}_{max}$ is the maximum value of signal and $\hat{x}_{min}$ is the minimum value of signal. Similarly, the signal de-normalization is performed as (12).

$$y_1(t) = \frac{(y(t)+1)(\hat{y}_{max} - \hat{y}_{min})}{2} + \hat{y}_{min} \tag{12}$$

Where $y(t)$ represents the neural network output before performing de-normalization and $y_1(t)$ is the final filtered signal after applying de-normalization process. The obtained signal is further processed through the deep learning-based model for peak detection.

2.2.2. QRS and R-peak detection

This section presents the proposed deep learning-based architecture for QRS complex detection. In this work, we have presented the combination of CNN, and Bi-LSTM. In Figure 5 shows the overall architecture of proposed ECG filtering and peak detection model.
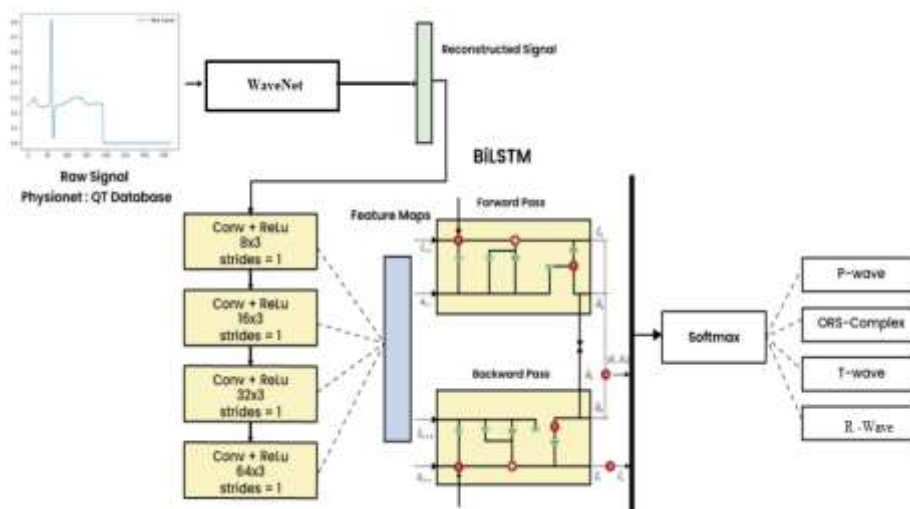

Figure 5. Proposed deep learning architecture for ECG filtering and peak detection

A. CNN layers

The CNN layers play important role in extracting the spatial and temporal data patterns with the help of four different factors (a) local connection (b) weight sharing (d) large number of filters and (e) reduced complexity of the network. In the given 1D-CNN, a sliding fixed window is used over the signal and the length of this widow is known as kernel size. The output of this layer represents the feature map. This process is based on the convolution operations which can be expressed as (13).

$$a_{ij}^m = \varphi\big(b_i + \sum_{k=1}^{M} w_{ik} x_{j+k-1}\big) = \varphi\big(b_i + w_i^T x_j\big) \tag{13}$$

Where a_{ij}^m represents the outcome of jth neuron of ith filter in m^{th} convolution layer, M represents the kernel size, φ is the activation function, b_i represents the bias, w denotes the shared weights and $x_j = [x_j, x_{j+1}, .., x_{j+M-1}]$ represents the inputs. The output of these neurons represents the filtered version of input data which is used to learn the features according to the sliding movement of kernel over input signal.

B. LSTM layer

In deep learning, the recurrent neural networks (RNNs) play important role in processing the sequential time-series data due to its capability to learn the sequential information. However, the traditional RNN based systems fail to maintain the long-term learning dependencies. In order to deal with this issue, researchers have developed a LSTM architecture which can tackle the issue of unstable gradient while maintaining long term dependencies.

The LSTM model has three main parts as (a) forget gate (b) input gate and (c) output gate. In LSTM, forget and input gate play important role in removing or adding the information to the memory block. This process of forget and input gate can be expressed as (14), (15).

$$f_n = \varphi\big(b_f + u_f^T a_n + w_f^T h_{n-1}\big) \tag{14}$$

$$i_n = \varphi(b_i + u_i^T a_n + w_i^T h_{n-1}) \tag{15}$$

Where a_n denotes the input to the LSTM, h_{n-1} represents the corresponding output sequence. The value of φ is characterized as $0 \leq \varphi(.) \leq 1$ which is used to control the contribution of each unit. Thus, the memory c_n can be updated as (16).

$$c_n = f_n c_{n-1} + i_n \tilde{c}_n \tag{16}$$

Where $\tilde{c}_n$ denotes the $tahnh$ function of weight and bias vectors, it can be expressed as (17).

$$\tilde{c}_n = \tanh(b_c + u_c^T a_n + w_c^T h_{n-1}) \tag{17}$$

The output vector of LSTM h_n is expressed as (18).

$$h_n = o_n \tanh(c_n) \tag{18}$$

Where o_n is the output gate given as: $o_n = \varphi(b_0 + w_0^T a_n + u_0^T h_{n-1})$ where u_o and w_o denotes the weight and b_0 is the bias of output gate. However, the complex nature of ECG signals causes difficulty in learning therefore currently, Bi-LSTM, a variant of LSTM is introduced which is capable to process the data in both backward and forward direction. Figure 6 shows the basic architecture of LSTM model. Based on these models, in algorithm 1 we present a complete of proposed filtering and peak detection scheme.
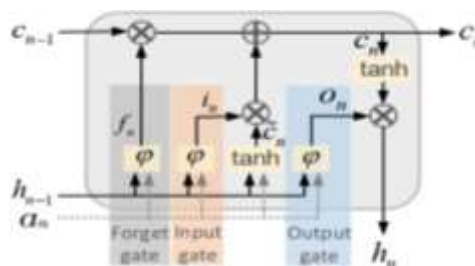

Figure 6. LSTM architecture

Algorithm 1. WaveConvBi-LSTM for ECG filtering and peak detection

```
  1.  Parameters: Input x (Signal Length, 1) and output yt (Signal Length, 4)
  2.  For each epoch do
  3.   If len(x) < 370 do:
  4.          Apply zero-padding
  5.  End if
# initiate Wavelet Transform and NN based denoising model
  6.  For each sample in X do:
  7.          Compute wavelet coefficients
  8.          Apply back propagation to update the weights as W(k + 1) = W(k) + η ∂J/∂W
  9.          Normalize and de-normalize the signal to get the filtered output
  10. End for
  11. End for
# Initialize the CNN-Bi-LSTM model
  12. For each conv layer do:
  13.         For each ECG sample in X do:
  14.         Compute aᵢⱼᵐ = φ(bᵢ + Σₖ₌₁ᴹ WᵢₖXₖⱼ + k − 1) = φ(bᵢ + WᵢᵀXⱼ)
  15. End for
# Initiate Bi-LSTM
  16. For each sample do:
  17.      apply forward processing model of Bi-LSTM as M¹ft = tanh(Wᵢ→ₕxₜ + W→ₕ→ₕ LSTM→₁ₜ₋₁ + b¹→ₕ)
  18.      apply backward processing of Bi-LSTM as M¹ft = tanh(Wᵢ←ₕxₜ + W←ₕ←ₕ LSTM←₁ₜ₊₁ + b¹←ₕ)
  19.   Compute final output y¹ₜ = tanh(W¹ₕ→₀ LSTM → M¹ₜ + W¹ₕ←₀LSTM ← M¹ₜ + b¹₀)
  20. End for
End for
```

C. Feature extraction and dimension reduction using PCA based feature selection

This section presents the proposed feature extraction module where we consider wavelet features as mentioned in previous section and incorporate the morphological feature extraction process to strengthen the feature modelling. According to the wavelet transform, we compute the scaling, wavelet, approximation and detailed coefficients which can be computed as (19)-(22).

$$s_{k,m} = \sum_{l=0}^{L_k-1} g_{k,l} x_{m-1} mod\ N \tag{19}$$

$$w_{k,m} = \sum_{l=0}^{L_k-1} h_{k,l} x_{m-1} mod\ N \tag{20}$$

$$a_{k,m} = \sum_{l=0}^{N-1} g_{k,l}^o s_{m+1} mod\ N \tag{21}$$

$$d_{k,m} = \sum_{l=0}^{N-1} h_{k,l}^o s_{m+1} mod\ N \tag{22}$$

Where s, w, a and d represents the scaling wavelet, approximation and detailed coefficients of the input signal.

In next phase, we consider RR interval features because it is considered as an important marker to discriminate between S and V bets from normal beats. In this work, we have used local, global, pre and post RR interval as combined features. These features can be computed as (23)-(26).

$$\text{Normalized RR}_{\text{Local}} \qquad \frac{RR_{\text{local}}}{\text{mean}(RR_{\text{local}})} \tag{23}$$

$$\text{Normalized RR}_{\text{global}} \qquad \frac{RR_{\text{global}}}{\text{mean}(RR_{\text{global}})} \tag{24}$$

$$\text{Normalized RR}_{\text{pre}} \qquad \frac{RR_{\text{pre}}}{\text{mean}(RR_{\text{pre}})} \tag{25}$$

$$\text{Normalized RR}_{\text{post}} \qquad \frac{RR_{\text{post}}}{\text{mean}(RR_{\text{post}})} \tag{26}$$

In next stage, we include high order statics features such as skewness and kurtosis which denotes the 3rd and 4th order statistics of signal. These features can be computed as (27), (28).

$$\text{Skewness} \qquad \frac{\sum_{i=1}^N (X_i - \bar{X})^3 / N}{s^3} \tag{27}$$

$$\text{Kurtosis} \qquad \frac{\sum_{i=1}^N (X_i - \bar{X})^4 / N}{s^4} - 3 \tag{28}$$

Finally, we incorporate PCA method for dimensionality reduction. According to this process, first of all mean is computed and subtracted from input ECG data. This can be expressed as (29).

$$Y = \frac{1}{N}\sum_{i=1}^{N}(X_i - \bar{X})   \tag{29}$$

Where N denotes the total number of samples and x_i represents the data matrix of aa segment of ECG beat. Based on this, the covariance matrix is computed as (30).

$$Cov = \frac{1}{N}\sum_{i=1}^{N}(X_i - \bar{X})(X_i - \bar{X})^T   \tag{30}$$

Further, the singular value decomposition method is performed on the obtained covariance matrix which generates the Eigen values. These values are arranged in the descending order and stored as coefficient. At this stage, the coefficients which have higher value than the certain threshold are selected as component of feature vector with reduced dimension. Thus, the final transformed data vector V can be denoted as (31).

$$V = PC^T X_i   \tag{31}$$

2.2.3. Classification model

The obtained feature vectors are trained by using supervised machine learning model. This section presents a brief model of support vector machine (SVM) and k-nearest neighbor (KNN) classifier models.

A. SVM model

It is a supervised classification model which is widely adopted to solve the statistical classification problems. It uses a hyperplane model to divide the data in to positive and negative sets with maximal margins. The dataset is considered in the form of pairs as $(a_1, y_1), (a_2, y_2), \dots, (a_N, y_N)$ and hyperplane represented in the form of quadratic problem as (32).

$$\max_{\alpha \geq 0} \begin{array}{c} \left(\sum_{i=0}^{l}\alpha - \frac{1}{2}\sum_{i,j=1}^{l}\alpha_i\alpha_j y_i y_j K(X_i, X_j)\right) \\ subject\ to\ \sum_{i=0}^{l}\alpha_i y_i = 0 \\ \alpha_i \leq C, i = 1,2,\dots,l \end{array}   \tag{32}$$

Here, X_i and X_j denotes the input feature vector whereas y_i and y_j denotes the corresponding class labels and $\alpha_i \geq$ is the Lagrangian multiplier where C is constant and K is the kernel function.

B. KNN model

KNN classifier is based on the instance-based learning approach which uses similarity index measurement to perform the classification. It determines the value of K in dataset training by using Euclidean distance measurement. This can be expressed as (33).

$$d(x_i, x_j) = \sqrt{\sum_{r=1}^{n}\left(a_r(x_i) - a_r(x_j)\right)^2}   \tag{33}$$

The local mean vector in KNN can be expressed as:

$$\gamma = \frac{1}{K}\sum_{x_i \in N_k(x)} y_i   \tag{34}$$

Where a_r denotes the value of rth variable γ is the local mean vector, $N_k(x)$ is the neighborhood instance of x element.

3.   RESULTS AND DISCUSSION

In this section, we evaluate the performance of proposed deep learning approach and compare the obtained performance with existing schemes. The proposed work has two main objectives as ECG signal denoising and peak detection. We compare the outcome of these two stages two show the robustness of proposed approach. We provided dataset sample used details.

3.1. Dataset details

MIT-BIH: is a publicly available arrhythmia dataset which contains 48 hours of two-channel ECG recording. These recordings were collected from 47 subjects from which 25 subjects are male and 22 subjects were female. All ECG signals are processed through the digitization process with a sampling rate of 360 elements per second per channel with bit-resolution of 11 over a space of 10 mV. This dataset is rearranged into four different categories based on the ANSI/AAMI standard. This mapping of ECG heartbeat according to these standards is presented in below given Table 1. Based on these standards, we focus on classifying the heart beats in five different categories as premature ventricular contraction (PVC), left bundle branch block (LBBB), right bundle branch block (RBBB), PACE, and atrial premature contraction (APC) to examine the heart condition.

Table 1. ECG heartbeat standards

ANSI standard	Symbol	MIT-BIH heart beat
Normal	N	Normal (N), Left (L), Right (R), Bundle branch block (e), atrial premature and escape beat (A)
Supra ventricular Ectopic beat	SVEB	S: supraventricular premature J: nodal premature and escape a: aberrated atrial premature
Ventricular ectopic Beat	VEB	PVC (V)
Fusion	F	Fusion (F)

3.2. Performance measurement parameters

As discussed before, the complete research performs signal filtering and peak detection tasks. The performance of these two tasks is measured with the help of different parameters. Signal filtering performance depends on the quality of reconstructed signal after removing the noise which can be measured in terms of improvement in SNR, cross correlation and PRD. Below given Table 2 shows the computations of these parameters.

Table 2. Performance measurement matrices: where $x(n)$ denotes the clean signal $z(n)$ is the noisy signal and $y(n)$ is the reconstructed output signal

Parameters	Output signal
Improvement in SNR	$SNR_{imp} = 10\, log_{10} \dfrac{\sum_{n=1}^{N}\big(z(n) - x(n)\big)^2}{\sum_{n=1}^{N}\big(y(n) - x(n)\big)^2}$
Cross-correlation	$\rho = 10\, log_{10} \dfrac{\sum_{n=1}^{N} x(n)y(n)}{\sqrt{\sum_{n=1}^{N}|x(n)|^2 \sum_{n=1}^{N}|y(n)|^2}}$
PRD	$PRD = \sqrt{\dfrac{\sum_{n=1}^{N}\big(x(n) - y(n)\big)^2}{\sum_{n=1}^{N}\big(x(n)\big)^2}}$

Similarly, we measure the classification performance where we have considered the 70% MIT-BIH dataset for training and 30% dataset for testing purpose. The obtained performance is measured in terms of accuracy, specificity, sensitivity and positive predictivity (PPV). In Table 3 shows the expressions to compute these parameters.

Table 3. Classification performance evaluation matrices

Parameter	Formula	Description
Sensitivity	$Se = \dfrac{1}{N}\sum_{i=1}^{N} \dfrac{(TP)_i}{(TP + FN)_i}$	It measures the average values of positive entities which are correctly classified.
Accuracy	$Acc = \dfrac{1}{N}\sum_{i=1}^{N} \dfrac{(TP + TN)}{(TP + FP + TN + FN)}$	It measures the rate of correctly classified entities out of total number of entities present in the testing set.
Positive predictivity	$PPV = \dfrac{1}{N}\sum_{i=1}^{N} \dfrac{(TP)_i}{(TP + FP)_i}$	It measures the positive prediction in correctly classified entities.

3.3. Filtering performance analysis

In order to analyze the filtering performance, we have considered different types of noises such as BW noise, EM noise, and MA noise. These noise parameters are scaled at the scale factor 1/16. Sampling and powerline frequency values are considered as 360 KHz and 60 KHz. In Figure 7 shows the sample clean signal. The original signal is contaminated by adding different types of noises. In Figure 8 shows the noisy signal samples obtained from NSTDB.
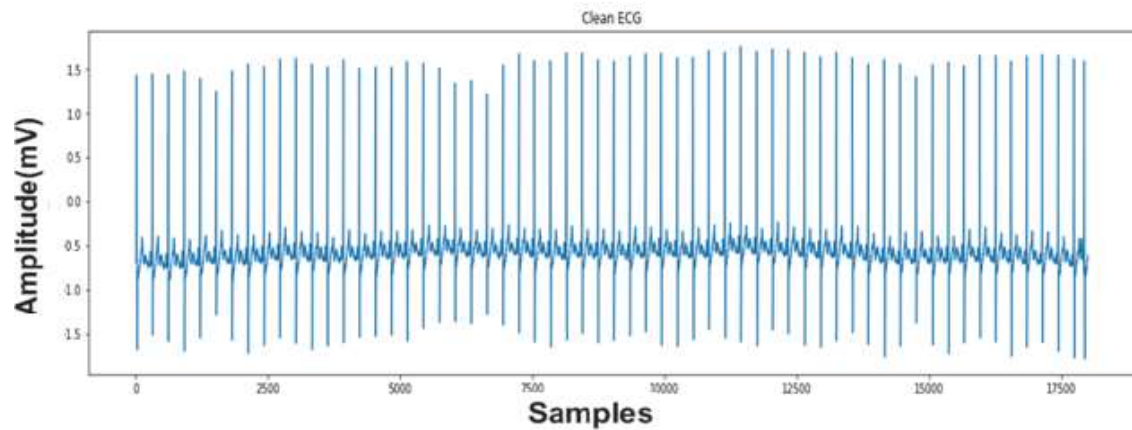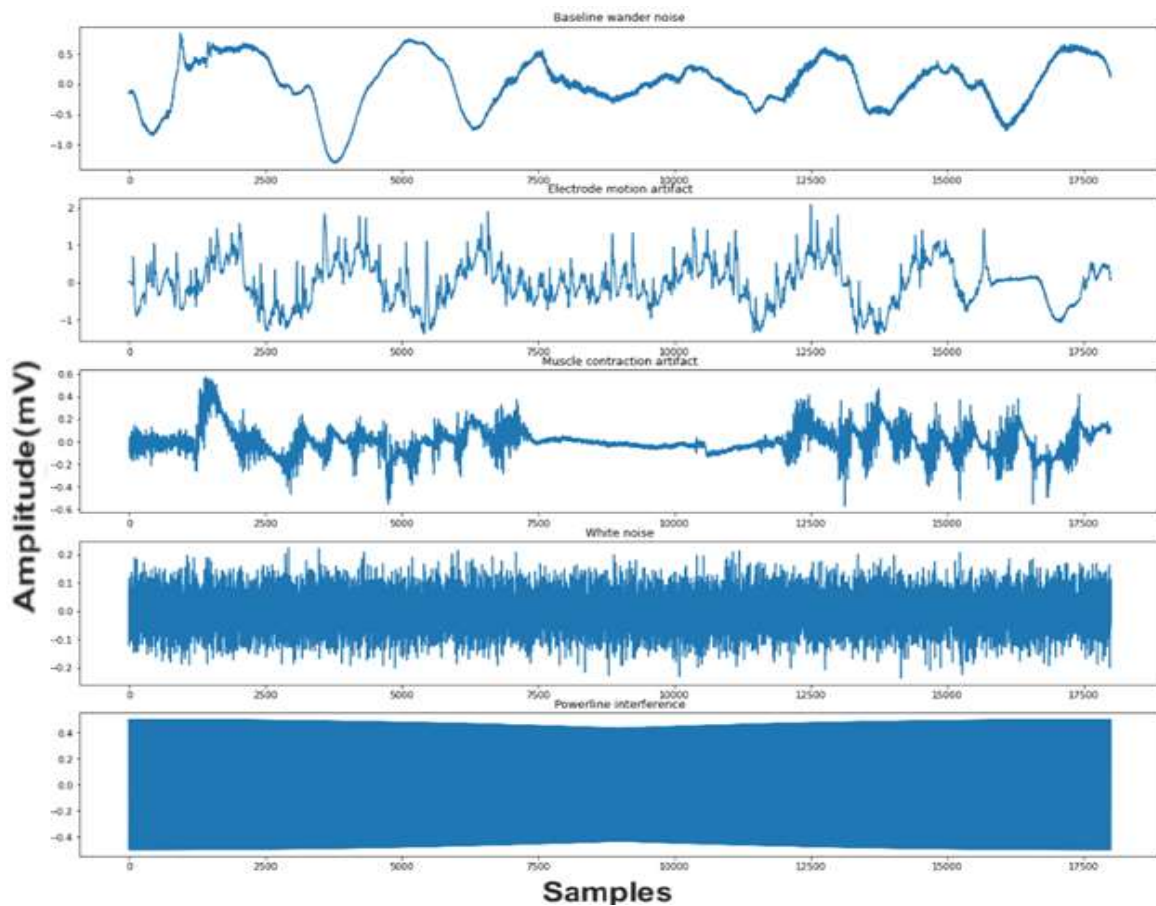

Figure 7. Clean ECG signal

Figure 8. Noisy signal samples

These noisy signals include baseline wander, motion artifact, white noise, and power line interference to contaminate the signal. These noisy signals are added to the clean signal to produce the final noisy signal which is presented in Figure 9. The noisy signal is processed through the proposed WaveNet model to obtain the filtered signal. The complete process is performed for 40 epochs where training loss and training MSE is obtained as 0.0023 and 0.0023. Similarly, the validation loss and validation MSE is obtained as 0.0027 and 0.0025, respectively. In Figure 10 shows the train and validation performance. Finally, in Figure 11 depicts the original signal and filtered signal to show the qualitative filtering performance.
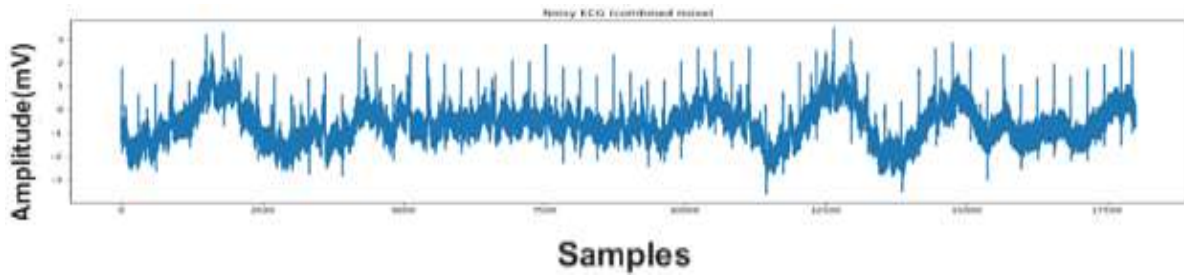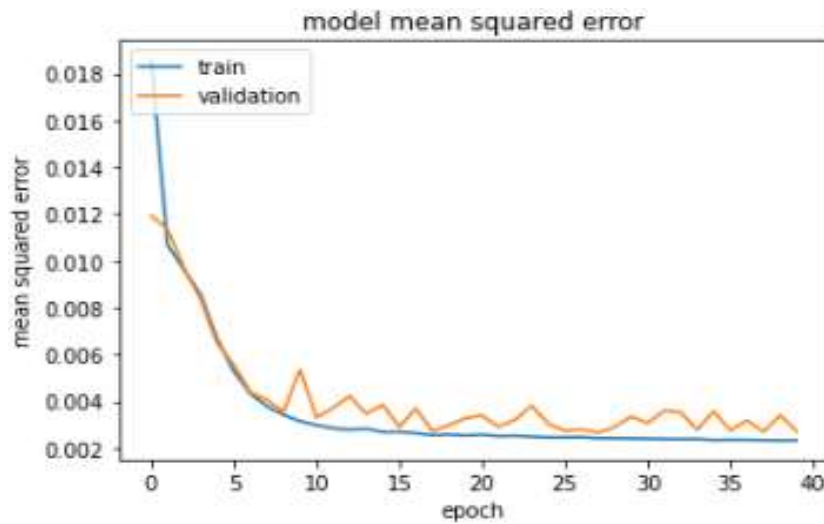

Figure 9. Noisy signal
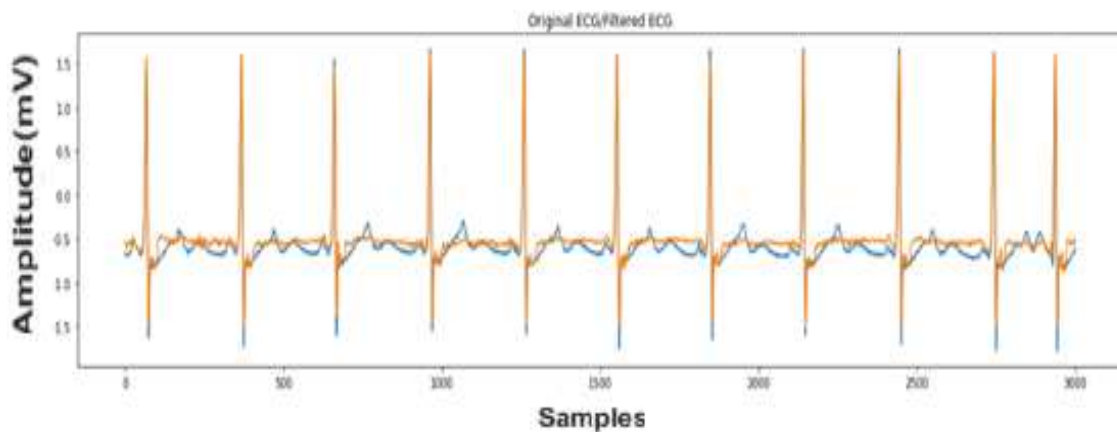

Figure 10. Training and validation performance

Figure 11. Original and filtered signal

Further, we consider PLI artefact with harmonics of 50-60 Hz and Baseline wander noise added to the clean ECG signals at different levels of SNR as -10 dB, -5 dB, 0 dB, 5 dB and 10 dB to ensure the robust performance of proposed model for wide range of noise power. The PLI harmonics is generated with the help of sinusoidal signal as $A(t) = A_0 \sin(2\pi f \times t)$ where f is the frequency. This sinusoidal signal is used to generate the 50 and 60 Hz noises.

In Table 4 show the obtained performance for 50 Hz PLI for varied SNR levels. According to this experiment, we measured the performance in terms of SNR improvement, cross-correlation and PRD for varied SNR levels in the presence of 50 Hz PLI noise. The overall analysis shows that the proposed approach achieves better denoising performance.

Table 4. Improvement SNR, cross-correlation and PRD performance for 50 Hz PLI

| | 5 dB | | | | | | 0 dB | | | | | | -5 dB | | | | | |
| | SNR | | ρ | | PRD | | SNR_i | | ρ | | PRD | | SNR | | P | | PRD | |
Record	LWT [21]	PS	LWT [21]	PS	LWT [21]	PS	LWT [21]	PS	LWT [21]	PS	LWT [21]	PS	LWT [21]	PS	LWT [21]	PS	LWT [21]	PS
100	11.25	13.20	0.986	0.988	16.75	18.50	15.25	16.30	0.9834	0.985	18.71	19.50	18.88	20.30	0.977	0.981	20.48	22.30
102	11.64	13.15	0.987	0.988	19.92	20.25	16.98	18.50	0.9887	0.989	20.66	22.30	21.17	22.10	0.986	0.987	20.72	21.10
103	12.07	14.5	0.989	0.987	10.83	12.50	16.73	18.60	0.9887	0.989	12.58	14.30	22.36	23.10	0.989	0.989	15.01	17.60
105	17.77	18.20	0.997	0.997	11.83	14.20	22.41	24.30	0.996	0.996	15.81	16.10	25.20	26.10	0.994	0.994	16.19	18.20
109	13.43	16.10	0.991	0.995	15.71	18.40	18.04	18.50	0.991	0.992	19.31	20.80	21.90	22.30	0.988	0.988	19.68	22.30
116	12.44	15.30	0.990	0.993	15.29	16.20	16.11	19.60	0.986	0.986	17.81	18.50	20.45	21.30	0.984	0.985	18.37	19.10
123	13.11	15.60	0.992	0.995	15.53	17.80	16.24	17.50	0.988	0.988	17.95	19.60	19.29	20.50	0.987	0.988	19.02	20.10
201	13.95	16.20	0.992	0.994	15.34	16.90	18.67	18.80	0.992	0.993	18.15	19.10	22.81	23.10	0.990	0.992	18.57	19.50
221	12.82	17.50	0.990	0.993	17.85	18.50	17.50	18.60	0.989	0.989	19.62	20.10	21.17	22.10	0.988	0.988	20.50	22.80
231	13.66	15.30	0.992	0.996	14.93	16.30	18.14	18.50	0.991	0.991	15.96	16.30	21.14	23.40	0.986	0.988	15.79	18.30
S0010	8.55	12.30	0.974	0.981	22.28	25.30	13.45	15.10	0.974	0.981	22.53	24.30	18.33	19.50	0.973	0.981	22.84	24.30
S0200	18.10	21.30	0.997	0.998	7.41	8.50	20.58	22.30	0.995	0.995	9.91	12.30	25.06	25.60	0.994	0.995	10.53	12.50
S0322	15.59	16.80	0.995	0.996	9.90	11.30	18.90	19.20	0.992	0.993	12.03	12.60	23.54	23.60	0.992	0.995	12.54	16.40
S0364	14.43	17.50	0.993	0.995	11.31	12.50	18.08	19.10	0.991	0.991	13.22	14.10	22.79	23.10	0.990	0.993	13.66	15.70
S0365	13.65	14.10	0.992	0.995	12.38	14.30	16.45	17.50	0.987	0.987	15.94	16.20	21.19	22.90	0.986	0.988	16.44	17.50
S0338	8.80	13.70	0.976	0.985	21.63	22.30	13.76	14.60	0.976	0.978	21.74	22.30	18.65	19.10	0.975	0.981	22.01	24.30
S0390	8.63	11.50	0.996	0.998	16.78	18.90	19.08	21.30	0.993	0.993	11.78	16.20	23.72	24.50	0.992	0.993	12.28	13.50

3.4. Peak detection performance analysis

In this subsection, we present the experimental analysis of proposed peak detection model and measure the performance in terms of true positive (TP), false negative (FN), false positive (FP), sensitivity and precision. Table 5 shows the obtained peak detection performance for MIT-BIH dataset.

Table 5. Peak detection performance analysis

| Record No. | Actual beats | Detected beats | | TP | | FN | | FP | | Sen (%) | | Pr (%) | |
		HSCW-BPF [24]	PS	HSCW-BPF [24]	PS	HSCW-BPF [24]	PS	HSCW-BPF [24]	PS	HSCW-BPF [24]	PS	HSCW-BPF [24]	PS
100	2273	2273	2273	2273	2273	0	0	0	0	100	100	100	100
101	1865	1865	1864	1863	1864	2	1	2	1	99.89	99.94	99.89	99.94
102	2187	2187	2187	2187	2187	0	0	0	0	100	100	100	100
103	2084	2081	2080	2079	2080	5	1	0	0	99.76	99.95	100	99.95
104	2229	2221	2225	2215	2225	14	4	6	0	99.37	99.80	99.72	99.82
105	2572	2571	2570	2567	2570	5	1	4	0	99.8	99.85	99.8	99.96
106	2027	2026	2025	2025	2025	2	0	1	1	99.90	99.90	99.95	99.90
109	2532	2531	2531	2531	2531	0	0	0	0	100	100	99.95	100
111	2124	2125	2124	2124	2124	0	0	1	0	100	100	99.95	100
112	2539	2540	2539	2539	2539	0	0	1	0	100	100	99.96	100
115	1953	1951	1951	1951		0	0	0	0	100	100	100	100
116	2412	2412	2412	2412	2412	0	0	0	0	100	100	100	100
117	1535	1535	1535	1535	1535	0	0	0	0	100	100	100	100
118	2278	2279	2278	2278	2278	0	0	1	1	100	99.95	99.95	99.85
119	1987	1988	1987	1987	1987	0	0	1	1	100	99.94	99.94	99.90
123	1518	1518	1518	1518	1518	0	0	0	0	100	100	100	100
124	1619	1619	1619	1619	1619	0	0	0	0	100	100	100	100
200	2601	2602	2601	2601	2601	0	1	1	0	100	99.95	99.96	99.90
210	2650	2650	2650	2649	2650	1	0	1	0	99.96	100	99.96	100

Further, we measure the overall performance in terms of sensitivity, precision and error rate performance for entire dataset and compared the existing performance as mentioned in [24]-[28]. In Table 6 shows the overall performance analysis. The comparative analysis shows that the existing schemes achieve reliable performance for MIT-BIH dataset however error rate remains the challenging issue in these methods whereas the proposed approach ensures reduced error rate with better precision and sensitivity.

Table 6. Comparative performance analysis for complete dataset

Technique	Precision	Sensitivity	Error rate
Zidelmal *et al.* [25]	99.64	99.82	0.540
Sabherwal *et al* [26]	99.90	99.90	0.160
Kaur *et al.* [24]	99.75	99.54	0.710
Phukpattaranont [27]	99.88	99.81	0.380
Sharma [28]	99.90	99.88	0.230
Kaur *et al.* [24]	99.93	99.95	0.117
Proposed	99.98	99.96	0.101

3.5. Classification performance

In this section, we present the classification performance by using decision tree, random forest, SVM and KNN classifiers. During training process, we divided the dataset as 70% for training and 30% testing. Below given Table 7 shows the comparative analysis of decision tree classifier.

Table 7. Classification performance for decision tree and random forest classifier

Beats	DT			RF		
	F1	Recall	Precision	F1	Recall	Precision
Normal	0.9757	0.9757	0.975	0.9860	0.992	0.9732
PVC	0.6400	0.6384	0.643	0.7533	0.609	0.9854
PACE	0.8568	0.8598	0.853	0.9284	0.882	0.9793
AFIB	0.5880	0.5925	0.585	0.7272	0.617	0.8849
APC	0.9417	0.9402	0.943	0.9687	0.944	0.9941

According to this experiment, the decision tree has reported highest precision as 94.3% for APC whereas lowest precision for AFIB as 58.5%. Further, we measure the performance for KNN classifier. In Table 7 demonstrates the obtained performance for different types of beats. According to Table 8, the SVM has reported highest precision for APC and lowest precision for AFIB as 99.5 and 75% whereas KNN has reported highest precision for APC as 99.41 and 76.29 for AFIB.

Table 8. Classification performance for SVM and KNN classifier

Beats	SVM			KNN		
	F1	Recall	Precision	F1	Recall	Precision
Normal	0.9824	0.9982	0.9672	0.9860	0.9946	0.9770
PVC	0.7120	0.5647	0.9631	0.7484	0.6420	0.8969
PACE	0.9110	0.8625	0.9667	0.9199	0.9012	0.9395
AFIB	0.5860	0.4814	0.7500	0.6936	0.6358	0.7629
APC	0.9516	0.9110	0.9950	0.9720	0.9508	0.9941

Further, in Figure 12 depicted and presented with confusion matrix and corresponding accuracy performance for different algorithms. Figure 12(a) decision tree, Figure 12(b) random forest, Figure 12(c) SVM, and Figure 12(d) KNN algorithms with accuracy=95.40, accuracy=97.47, accuracy=96.80 and accuracy=97.36 respectively. According to this experiment, the class 1 has highest instances where RF classifier has predicted the highest true positives as 18103 for class 1, the KNN has highest accuracy for class 2, 3, 4, and 5 because it has predicted highest TPs as 357, 1305, 103, and 1529, respectively.
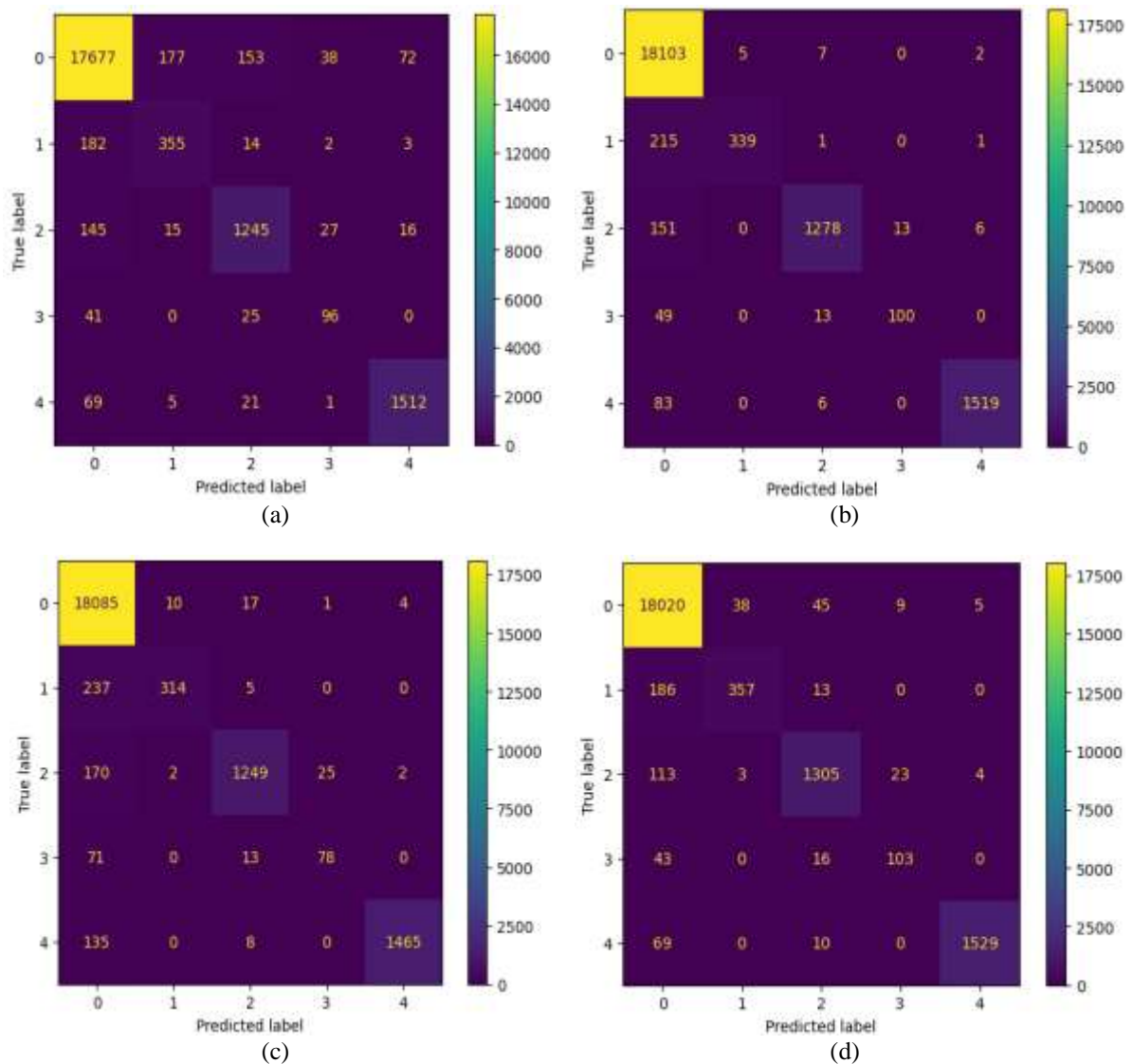
Figure 12. Confusion matrix: (a) DT (accuracy=95.40), (b) RF (accuracy=97.47), (c) SVM (accuracy=96.80), and (d) KNN (accuracy=97.36)

4. CONCLUSION

This research has delved into the realm of portable health monitoring systems, particularly focusing on the crucial aspect of cardiovascular disease detection using ECG. We have demonstrated the significance of incorporating advanced signal processing techniques, such as wavelet transform, neural networks, and Bi-LSTM networks, to enhance the accuracy of ECG signal analysis. Through our investigation, we have identified the pressing need for robust methods to filter ECG signals and detect abnormalities accurately, given the prevalence of signal contamination during acquisition. Our proposed combined approach, augmented by PCA-based dimensionality reduction and supervised machine learning classification models, has yielded impressive performance metrics, as evidenced by our evaluation on the MIT-BIH dataset where average precision and sensitivity performance is obtained as 99.98% and 99.96%, respectively. These findings hold profound implications for both the research field and our community. Firstly, they underscore the potential of advanced signal processing techniques in revolutionizing portable health monitoring systems, particularly in mitigating the risks associated with cardiovascular diseases, a leading cause of mortality among the elderly. By enabling early detection and intervention, our methodology can significantly improve outcomes and enhance the quality of life for individuals at risk of heart-related issues. In essence, our findings signify a significant advancement in the field of portable health monitoring systems, offering promising solutions to address critical healthcare challenges. By leveraging advanced signal processing

techniques and machine learning algorithms, we pave the way for transformative innovations that have the potential to positively impact the lives of individuals worldwide, ushering in a new era of proactive and personalized healthcare.

REFERENCES

[1] A. S. Abdulbaqi, A. J. Obaid, and M. H. Abdulameer, "Smartphone-based ECG signals encryption for transmission and analyzing via IoMTs," *Journal of Discrete Mathematical Sciences and Cryptography*, vol. 24, no. 7, pp. 1979–1988, Oct. 2021, doi: 10.1080/09720529.2021.1958996.

[2] M. Elgendi, "Less is more in biosignal analysis: compressed data could open the door to faster and better diagnosis," *Diseases*, vol. 6, no. 1, p. 18, Feb. 2018, doi: 10.3390/diseases6010018.

[3] S. P. Kishore and M. D. Michelow, "The global burden of disease," *Public Health in the 21st Century: Volume 1-3*, 2010. .

[4] X. Wang, Y. Zhou, M. Shu, Y. Wang, and A. Dong, "ECG baseline wander correction and denoising based on sparsity," *IEEE Access*, vol. 7, pp. 31573–31585, 2019, doi: 10.1109/ACCESS.2019.2902616.

[5] B. Chen, Y. Li, X. Cao, W. Sun, and W. He, "Removal of power line interference from ECG signals using adaptive notch filters of sharp resolution," *IEEE Access*, vol. 7, pp. 150667–150676, 2019, doi: 10.1109/ACCESS.2019.2944027.

[6] M. F. Issa, G. Tuboly, G. Kozmann, and Z. Juhasz, "Automatic ECG artefact removal from EEG signals," *Measurement Science Review*, vol. 19, no. 3, pp. 101–108, Jun. 2019, doi: 10.2478/msr-2019-0016.

[7] S. Chatterjee, R. S. Thakur, R. N. Yadav, L. Gupta, and D. K. Raghuvanshi, "Review of noise removal techniques in ECG signals," *IET Signal Processing*, vol. 14, no. 9, pp. 569–590, Dec. 2020, doi: 10.1049/iet-spr.2020.0104.

[8] S. I. Haider and M. Alhussein, "Detection and classification of baseline-wander noise in ECG signals using discrete wavelet transform and decision tree classifier," *Elektronika ir Elektrotechnika*, vol. 25, no. 4, pp. 47–57, Aug. 2019, doi: 10.5755/j01.eie.25.4.23970.

[9] D. Acharya, A. Rani, S. Agarwal, and V. Singh, "Application of adaptive Savitzky–Golay filter for EEG signal processing," *Perspectives in Science*, vol. 8, pp. 677–679, Sep. 2016, doi: 10.1016/j.pisc.2016.06.056.

[10] S. Sarafan *et al.*, "A novel ECG denoising scheme using the ensemble Kalman filter," in *Proceedings of the Annual International Conference of the IEEE Engineering in Medicine and Biology Society, EMBS*, Jul. 2022, vol. 2022-July, pp. 2005–2008, doi: 10.1109/EMBC48229.2022.9871884.

[11] A. K. Dwivedi, H. Ranjan, A. Menon, and P. Periasamy, "Noise reduction in ECG signal using combined ensemble empirical mode decomposition method with stationary wavelet transform," *Circuits, Systems, and Signal Processing*, vol. 40, no. 2, pp. 827–844, Feb. 2021, doi: 10.1007/s00034-020-01498-4.

[12] Y. Ding *et al.*, "Adaptive recursive least squares denoising in ventricular fibrillation ECG signals," *Advanced Sensor Research*, vol. 2, no. 5, May 2023, doi: 10.1002/adsr.202200035.

[13] E. Fotiadou and R. Vullings, "Multi-channel fetal ECG denoising with deep convolutional neural networks," *Frontiers in Pediatrics*, vol. 8, Aug. 2020, doi: 10.3389/fped.2020.00508.

[14] E. Fotiadou, T. Konopczyński, J. Hesser, and R. Vullings, "End-to-end trained encoder-decoder convolutional neural network for fetal electrocardiogram signal denoising," *Physiological Measurement*, vol. 41, no. 1, p. 015005, Feb. 2020, doi: 10.1088/1361-6579/ab69b9.

[15] H. T. Chiang, Y. Y. Hsieh, S. W. Fu, K. H. Hung, Y. Tsao, and S. Y. Chien, "Noise reduction in ECG signals using fully convolutional denoising autoencoders," *IEEE Access*, vol. 7, pp. 60806–60813, 2019, doi: 10.1109/ACCESS.2019.2912036.

[16] J. Jang, S. Park, J. K. Kim, J. An, and S. Jung, "CNN-based two step R peak detection method: combining segmentation and regression," in *Proceedings of the Annual International Conference of the IEEE Engineering in Medicine and Biology Society, EMBS*, Jul. 2022, vol. 2022-July, pp. 1910–1914, doi: 10.1109/EMBC48229.2022.9871227.

[17] M. U. Zahid *et al.*, "Robust R-peak detection in low-quality holter ECGs using 1D convolutional neural network," *IEEE Transactions on Biomedical Engineering*, vol. 69, no. 1, pp. 119–128, Jan. 2022, doi: 10.1109/TBME.2021.3088218.

[18] A. Kumar, H. Tomar, V. K. Mehla, R. Komaragiri, and M. Kumar, "Stationary wavelet transform based ECG signal denoising method," *ISA Transactions*, vol. 114, pp. 251–262, Aug. 2021, doi: 10.1016/j.isatra.2020.12.029.

[19] H. D. Hesar and M. Mohebbi, "An adaptive Kalman filter bank for ECG denoising," *IEEE Journal of Biomedical and Health Informatics*, vol. 25, no. 1, pp. 13–21, Jan. 2021, doi: 10.1109/JBHI.2020.2982935.

[20] N. Mourad, "ECG denoising based on successive local filtering," *Biomedical Signal Processing and Control*, vol. 73, p. 103431, Mar. 2022, doi: 10.1016/j.bspc.2021.103431.

[21] S. A. Malik, S. A. Parah, H. Aljuaid, and B. A. Malik, "An iterative filtering based ECG denoising using lifting wavelet transform technique," *Electronics (Switzerland)*, vol. 12, no. 2, p. 387, Jan. 2023, doi: 10.3390/electronics12020387.

[22] M. Gabbouj *et al.*, "Robust peak detection for holter ECGs by self-organized operational neural networks," *IEEE Transactions on Neural Networks and Learning Systems*, vol. 34, no. 11, pp. 9363–9374, Nov. 2023, doi: 10.1109/TNNLS.2022.3158867.

[23] J. Laitala *et al.*, "Robust ECG R-peak detection using LSTM," in *Proceedings of the ACM Symposium on Applied Computing*, Mar. 2020, pp. 1104–1111, doi: 10.1145/3341105.3373945.

[24] A. Kaur, A. Agarwal, R. Agarwal, and S. Kumar, "A novel approach to ECG R-peak detection," *Arabian Journal for Science and Engineering*, vol. 44, no. 8, pp. 6679–6691, Aug. 2019, doi: 10.1007/s13369-018-3557-8.

[25] Z. Zidelmal, A. Amirou, M. Adnane, and A. Belouchrani, "QRS detection based on wavelet coefficients," *Computer Methods and Programs in Biomedicine*, vol. 107, no. 3, pp. 490–496, Sep. 2012, doi: 10.1016/j.cmpb.2011.12.004.

[26] P. Sabherwal, M. Agrawal, and L. Singh, "Automatic detection of the R peaks in single-lead ECG signal," *Circuits, Systems, and Signal Processing*, vol. 36, no. 11, pp. 4637–4652, Nov. 2017, doi: 10.1007/s00034-017-0537-2.

[27] P. Phukpattaranont, "QRS detection algorithm based on the quadratic filter," *Expert Systems with Applications*, vol. 42, no. 11, pp. 4867–4877, Jul. 2015, doi: 10.1016/j.eswa.2015.02.012.

[28] T. Sharma and K. K. Sharma, "QRS complex detection in ECG signals using locally adaptive weighted total variation denoising," *Computers in Biology and Medicine*, vol. 87, pp. 187–199, Aug. 2017, doi: 10.1016/j.compbiomed.2017.05.027.

BIOGRAPHIES OF AUTHORS

Raghavendra Badiger ⓘ 🗗 sc ᗡ is IT Manager- Data Services at Voya India, Raghavendra Badiger is presently working in Voya India Private Limited at Bengaluru as Manager-Data services. He holds Master Degree in Computer Science and Engineering and currently pursuing Ph.D. in REVA University. He is having 16+ years of IT experience in data services. His research areas are machine learning, deep learning and Gen-AI. He has taken multiple automation initiatives in Data and Data Testing areas within Voya Organization to save efforts and process optimization. Recently published paper on ECG noise filter using deep learning and submitted couple of conference papers of heart decease and ECG filtering. He can be contacted at email: raghavendra.badiger1@gmail.com.

Prabhakar Manickam ⓘ 🗗 sc ᗡ is presently working as Professor in School of Computer Science and Engineering, REVA University Bangalore with an aim of designing a project for farmers in India to cultivate appropriate crop in appropriate time for better yield. He has published about 15 patents and grants in various fields including internet of things, image processing, education, and security in WSNs. He was awarded 'Excellence in Research', by Novel Research Academy, Puducherry, India. He has delivered many guest lectures on internet of things in `border security force signal training school (BSF-STS) for Officers' - Bangalore. He recently organized an International Workshop on "Cyber Security" in collaboration with Florida International University, U.S.A., at REVA University, Bangalore, India, and many such workshops, webinars and seminars in association with NIT- Warangal and international organizations such as IBM, Cisco and Kirusa Inc. He has published about 50 research articles in blind- peer reviewed International and National Journals which are Scopus and WoS indexed with about 980 citations at present. He has successfully guided four Ph.D. Research Scholars and six are pursuing currently. Besides these achievements, he has attended many Workshops and Seminars conducted by IBM, Intel, and Cisco focusing on Microcontroller Boards that are very commonly used in IoT Applications. He is continuously contributing exceptionally as Central Evaluator and Judge in "Smart India Hackathon" organized by Ministry of HRD, India. His area of research is IoT, WSN, medical image processing and natural language processing and artificial intelligence. He can be contacted at email: prabhakar.m@reva.edu.in.